

IDENTIFICATION AND PRESERVATION OF SURFACE FEATURES

Timothy J. Baker

Dept. of MAE, Princeton University, Princeton, NJ, U.S.A. baker@tornado.princeton.edu

ABSTRACT

A surface is often approximated by a network of triangular facets. In the absence of a precise mathematical description of the underlying surface all information about surface properties such as smoothness and curvature must be inferred from the triangulation itself. Enrichment and coarsening of the surface geometry, for example, can only be carried out if singular features, where C^1 continuity is lost, are properly accounted for. In the absence of a well defined surface geometry it is necessary to extract these features and establish suitable data structures so that the features persist after enrichment and/or coarsening of the triangulation. This paper describes a feature extraction scheme that is based on estimates of the local normals and principal curvatures at each mesh point. The feature extraction scheme has been combined with an algorithm that adapts a tetrahedral mesh by the selective enrichment and coarsening of both the volume and surface triangulation.

Keywords: surface triangulation, feature extraction, surface projection

1. INTRODUCTION

Mesh enrichment, coarsening and mesh point movement are fundamental operations employed by mesh adaptation algorithms. The application of these operations on a domain boundary involves a modification of the surface triangulation and care must be taken to ensure that the integrity of the boundary surface is preserved. Sometimes the surface is defined analytically by a number of patches with C^1 continuity inside each patch but with a possible loss of C^1 continuity along patch boundaries where corners, ridges and other singular curves may exist. In such cases, the actual surface is unambiguously defined and the projection of a new mesh point onto the surface can be obtained by interrogating the CAD representation. There are, however, many situations when a precise mathematical description of the surface is not known or not available. The surface may be defined simply as a point cloud obtained by a laser scanning device, or as collection of curves obtained from the segmentation of an MRI scan. A surface triangulation of the point positions then provides all the available infor-

mation about the surface, and any assessment of the underlying surface properties must be extracted from the surface triangulation.

This paper considers the problem of extracting an adequate knowledge base from an existing surface triangulation. The basic premise is that any reasonable surface is made up of several smooth regions where a well defined tangent plane can be defined together with a number of singular curves along which C^1 continuity may be lost. Any mechanical or other man-made object falls into this category, as do most biological specimens that may arise from medical applications requiring the visualization of organs or other body structures. Any surface that is essentially random or chaotic in nature would not fit into this category but, in such cases, the simplest form of interpolation or point projection would probably suffice.

Early work on feature identification was mostly associated with research into pattern recognition [1]. More recently, techniques for manipulating and coarsening surface triangulations have received considerable attention [2, 3] This in turn has stimulated interest in

feature identification for surface triangulations [4, 5].

The work described in this paper was motivated by the need to manipulate and deform tetrahedral meshes whose boundaries are defined by conforming surface triangulations. The examples presented herein illustrate the coarsening and refinement of tetrahedral meshes whose boundaries are defined by surface triangulations containing a number of features. Preservation of the overall surface shape under the action of mesh coarsening or refinement can only be achieved if the surface features are accurately detected and accounted for during mesh modification.

The following section describes the assumptions that have been made about the structure of any singular features and the rules that have been developed to extract them. The feature extraction rules depend in part on estimates of the principal curvatures at any point on the surface which in turn require an estimation of the normal at each point. The procedure for estimating the normal and curvatures at each point of the surface triangulation are described in sections 3 and 4. This is followed by a discussion of point projection on both smooth regions and along singular curves with a number of examples to illustrate the application of these ideas.

2. FEATURE IDENTIFICATION

It is assumed that any feature consists of a concatenation of two or more edges, each of which meets certain requirements that qualify the edge to be part of a feature. A feature can therefore be regarded as a simple, possibly closed, polygonal curve whose straight line segments are formed by qualifying edges. The condition for an edge to qualify as part of a feature is to some extent subjective and so a few user specified parameters are required to determine what constitutes a valid feature edge. The rules that follow attempt to keep the number of user specified parameters as small as possible while exploiting reasonable assumptions about the geometric characterization of features as singular curves separating regions where the surface can be regarded as smoothly varying.

2.1 Edge Classification

It is assumed that every triangle T in the surface triangulation τ has an orientation defined by an outward pointing normal and that every edge e is incident to at most two triangles in τ . Let θ_e be the dihedral angle between the normals associated with the triangles incident to e ; if only one triangle is incident to e then θ_e is assigned the value zero.

A feature can arise in different ways. Consider, for example, an object such as a box that is formed by

six planar regions. It is evident that any feature line corresponds to the intersection of two incident planar regions. The dihedral angle θ_e of any edge e in the triangulation that lies on the interior of a planar region is zero while any edge lying along a feature is characterized by a non-zero value of θ_e . In this case, the angle θ_e is sufficient to determine all feature lines no matter how coarse or fine the surface triangulation may be. On the other hand, for an entirely smooth object the maximum dihedral angle θ_{max} can be made arbitrarily small if the surface triangulation is refined in a manner that maintains a lower bound on the triangle aspect ratio. For an object such as a high aspect ratio ellipsoid, for example, it is often desirable to characterize points where the curvature is very high as lying on a feature, no matter how fine the surface triangulation may be.

In other words, an edge can belong to a feature if it possesses one or both of the following properties

(a) the dihedral angle θ_e is large, and/or (b) the principal curvatures κ_1 and κ_2 at either endpoint of the edge satisfy $\max(|\kappa_1|, |\kappa_2|) \gg 1$ and $\min(|\kappa_1|, |\kappa_2|) \ll 1$, and in addition, the edge is close to the direction of curvature associated with $\min(|\kappa_1|, |\kappa_2|)$.

The edges are first classified based on two threshold values of θ_e . Let θ_{avr} represent the mean value $\langle \theta_e \rangle$ over all edges e and let $\sigma^2 = \langle \theta_e^2 \rangle - \theta_{avr}^2$ be the variance of the edge angles for the surface mesh. The threshold angle θ_s is set equal to $\theta_{avr} + \mu\sigma$ where μ is a user specified parameter. The restriction $\mu < 1$ ensures that at least one edge satisfies $\theta_e \geq \theta_s$ no matter how fine the triangulation may be.

Let λ be another user defined parameter that satisfies $\lambda > 1 > \mu$ and let ϕ be a user defined angle. Then define the second threshold angle to be

$$\theta_d = \max(\phi, \min(\theta_{max} - \sigma, \theta_{avr} + \lambda\sigma)) \quad (1)$$

If $\phi > \theta_{max}$ then no edges will have dihedral angles greater than the threshold value θ_d , a situation that may occur for a very fine triangulation of a smooth object. If the triangulation is fairly coarse, however, then estimates of the principal curvatures and their directions may not be accurate enough to apply criterion (b) above. In this case, the condition that $\theta_e > \theta_d$ is considered sufficient to identify a feature edge. These considerations prompt the following,

Definition Given constants θ_d and θ_s such that $\theta_d > \theta_s$, an edge e is said to be **dominant** if $\theta_e > \theta_d$; **sub-dominant** if $\theta_d \geq \theta_e > \theta_s$ and e is incident to at least one dominant or sub-dominant edge; **non-dominant** otherwise, in other words, if $\theta_e \leq \theta_s$ or if $\theta_d \geq \theta_e > \theta_s$ and e is not incident to a dominant or sub-dominant edge.

Let E_d be a list of all dominant edges, ordered according to dihedral angle, with the edge whose dihedral angle is largest appearing first. Let E_s be a list of all sub-dominant edges that is also arranged in order of decreasing dihedral angle. Any dominant edge $e \in E_d$ is considered to be a feature edge by virtue of condition (a) above. A sub-dominant edge $e \in E_s$ will qualify to be a feature edge if it meets the additional requirement specified in condition (b).

A somewhat similar form of edge classification has previously been presented by Jiao and Heath[5] who define the concepts of strong and relatively strong edges which closely resemble the dominant and sub-dominant edges defined above. The application of condition (b) and the associated test to determine whether a candidate sub-dominant edge is aligned with a particular curvature direction is believed to be a novel aspect of the feature detection scheme presented in this paper.

2.2 Point Classification

For each point P in the surface triangulation let X_P be the set of points that are edge incident to P (*i.e.* $Q \in X_P$ if there exists an edge whose endpoints are P and Q). Let $m = \text{card } X_P$ and $d(P, Q)$ be the Euclidean distance between P and Q . The average edge length L_P associated with P is then defined as the average edge length over X_P , or

$$L_P = \frac{1}{m} \sum_{Q \in X_P} d(P, Q) \quad (2)$$

Let κ_1 and κ_2 be the principal curvatures at P and let j be the index for which $|\kappa_j| = \min(|\kappa_1|, |\kappa_2|)$. Define \mathbf{t}_1 , respectively \mathbf{t}_2 , as the orthogonal unit vectors lying in the tangent plane at P that are aligned with the directions corresponding to the curvatures κ_1 and κ_2 . Now let \mathbf{n} to be the unit normal at P so that $\{\mathbf{t}_1, \mathbf{t}_2, \mathbf{n}\}$ is an orthonormal triad of vectors associated with the point P . A normalized Gaussian curvature is then defined for each point P as $G_P = \kappa_1 \kappa_2 L_P^2$. Let G_{max} and G_{min} be the maximum and minimum values of the normalized Gaussian curvature over all surface mesh points.

Definition

(i) If $\frac{G_{max} - G_{min}}{G_{max}} \leq \delta$ where δ is a user specified parameter then all points are said to be **smooth**.

(ii) If $\frac{G_{max} - G_{min}}{G_{max}} > \delta$ then the point P is said to be an **apex** point if more than two incident edges are dominant.

Part (i) of this definition is intended to identify objects whose boundaries can be regarded as devoid of features. Without this filter it is possible that some spurious features could be identified on objects that are inherently featureless. A sphere would clearly fall

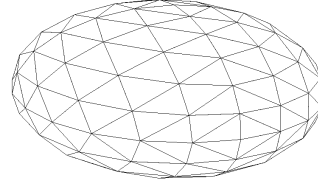


Figure 1: Ellipsoid with ratio of minor to major axis equal to 0.5 has no features.

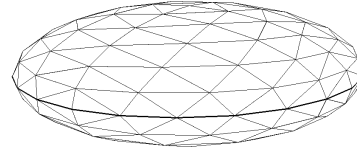


Figure 2: Ellipsoid with ratio of minor to major axis equal to 0.35 has a closed loop feature.

into this category. An ellipsoid, however, could be regarded as having a closed loop feature in the plane of symmetry normal to the minor axis if the ratio of the minor to major axis is small enough. This is illustrated in figures 1 and 2 which show two ellipsoids whose aspect ratios (length of minor axis divided by length of major axis) are 0.5 and 0.35 respectively. With the choice $\delta = 0.2$ the larger aspect ratio ellipsoid is considered to be featureless while the smaller aspect ratio ellipsoid is regarded as having some non-smooth points. A closed loop feature curve has been identified for this case and the edges that belong to this feature are indicated in figure 2 by thicker lines.

If the maximum and minimum values of normalized Gaussian curvature satisfy condition (ii) of this definition then a search for possible feature curves is carried out. Take the first member e_d of E_d and find the sequence of edges, according to the rules given in subsection 2.3, that together with e_d form a feature curve. Then find the next edge in E_d that has not already been assigned to a feature curve and repeat the process to find a new feature curve.

When the list of edges in E_d has been exhausted the feature assembly procedure continues by examining, in a similar manner, edges in E_s that have not already been assigned to a feature curve. The construction of feature curves stops when the list of edges in E_s has been exhausted.

Definition

Any non-apex point P that lies on a feature curve is said to be a **ridge** point. Any point P that does not lie on a feature curve is said to be a **smooth** point.

The distinction between apex points and ridge points plays an important role in the process that identifies individual features. An apex point, for example, must always lie at the terminus of a feature and cannot appear as an interior point. When coarsening a surface triangulation, it is permissible to remove a ridge point P provided the coarsened triangulation contains an edge connecting the feature points that occur immediately before and after P in the unmodified triangulation. It is also permissible to create a new ridge point by inserting a surface point at the midpoint of a feature edge. The set of apex points, however, should generally be conserved; none should be removed during coarsening and none should be introduced during enrichment.

2.3 Feature Detection and Classification

Given a candidate edge e_1 from either E_d or E_s , choose one endpoint, say P_1 , and then check whether any other edge incident to P_1 is a valid next feature edge. Let U be the set of all dominant edges e , excluding e_1 , that are incident to P_1 and let V be the set of all sub-dominant edges, excluding e_1 , that are incident to P_1 . The condition for being a valid next feature edge e_2 is based on the following criteria;

- (i) If U is not empty choose e_2 to be the member of U whose dihedral angle is largest.
- (ii) If U is empty but V is not empty let e_m be the member of V whose dihedral angle is largest. If e_m is also the member of V that is most closely aligned with the direction \mathbf{t}_j of the minimum of the absolute values of the principal curvatures κ_1 and κ_2 choose e_m as the next feature edge e_2 .

If a next feature edge e_2 has been found let P_2 be the endpoint of e_2 that is opposite P_1 . Replace e_1 by e_2 and P_1 by P_2 and repeat the above search to find a next feature edge. The search stops if a point found in the search coincides with the starting point (this indicates a closed feature curve), or if both terminal points of the feature have been found. A feature terminus has been reached if in test (ii) edge e_m is not the same as the edge in V that is most closely aligned with the direction \mathbf{t}_j , or if both sets U and V are empty, or if

P_2 is an apex point.

After completing the search for feature edges in one direction (*i.e.* if a feature terminus point has been found and the feature is not a closed loop) the process is repeated starting with the original edge e_1 and the edge endpoint opposite the starting point P_1 until the second feature terminal point has been found. The feature points and edges are then sorted in order starting from one terminal point and ending at the second terminal point. A data structure is created to link each point in the feature to its successor and antecedent in the feature.

3. SURFACE NORMAL ESTIMATION

The normal at a mesh point P is often computed by averaging the normals of the incident triangles. An alternative approach that appears to be less sensitive to the shape and connectivity of the incident triangles is based on finding the plane, passing through the barycenter of the set of points X_P , that minimizes the sum of the squared distances from the plane of each point in X_P . Let $\mathbf{x}_Q \in X_P$, be the position vector associated with point Q and let

$$\bar{\mathbf{x}} = \frac{1}{m} \sum_{Q \in X_P} \mathbf{x}_Q \quad (3)$$

be the barycenter of X_P . If a plane through $\bar{\mathbf{x}}$ has an orientation given by the unit normal \mathbf{n} then the distance of Q from the plane is given by $h_Q = \mathbf{n}^T(\mathbf{x}_Q - \bar{\mathbf{x}})$. It follows that the error to be minimized is given by

$$E(\mathbf{n}) = \sum_{Q \in X_P} h_Q^2 \quad (4)$$

Thus $E(\mathbf{n}) = \mathbf{n}^T \mathbf{A} \mathbf{n}$ where

$$\mathbf{A} = \sum_{Q \in X_P} (\mathbf{x}_Q - \bar{\mathbf{x}})(\mathbf{x}_Q - \bar{\mathbf{x}})^T \quad (5)$$

is a symmetric positive semi-definite matrix.

Let $\mathbf{n}^T = (u, v, w)$. The required orientation of the plane through $\bar{\mathbf{x}}$ is found by minimizing $E(\mathbf{n})$ with respect to the variables u, v and w subject to the constraint that $\mathbf{n}^T \mathbf{n} = 1$. Introducing a Lagrange multiplier λ , the function to be minimized is given by

$$\tilde{E}(\mathbf{n}) = \mathbf{n}^T \mathbf{A} \mathbf{n} - \lambda \mathbf{n}^T \mathbf{n} \quad (6)$$

which leads to the eigenvalue problem

$$\mathbf{A} \mathbf{n} = \lambda \mathbf{n} \quad (7)$$

The eigenvalues λ of \mathbf{A} correspond to level curves of the quadric $E(\mathbf{n})$ and the minimum value of $E(\mathbf{n})$ is given by the smallest eigenvalue λ_{min} . The estimated

normal at P is then chosen to be the eigenvector associated with λ_{min} . This minimization procedure determines the alignment of the vector \mathbf{n} but not the sign of \mathbf{n} which can, however, be obtained from the known orientation of the triangles incident to P .

If all points in X_P lie on a plane whose orientation is given by the unit vector \mathbf{p} then this procedure will compute \mathbf{p} as the estimated normal for the point P . This can be seen by observing that in this case

$$(\mathbf{x}_Q - \bar{\mathbf{x}})^T \mathbf{p} \equiv \mathbf{p}^T (\mathbf{x}_Q - \bar{\mathbf{x}}) = 0, \quad \forall Q \in X_P \quad (8)$$

It follows that \mathbf{p} is in the null-space of A and is therefore an eigenvector whose associated eigenvalue is zero. Since all eigenvalues of A are non-negative, $\lambda_{min} = 0$ in this case and \mathbf{p} will be the estimated normal at the point P .

It can be shown that the sum of the vector areas of the triangles incident to P will also return the vector \mathbf{p} for the case when all points in X_P lie on a plane normal to \mathbf{p} . The minimization procedure, however, appears to be less sensitive to perturbations in the positions of the points in X_P .

A different minimization procedure for estimating the normal at P computes the vector that minimizes the square of the angles between \mathbf{n} and the edges incident to P .

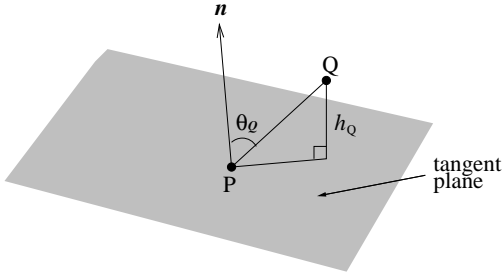


Figure 3: Tangent plane fit through P to minimize square angle sum.

Define

$$\hat{h}_Q = \frac{h_Q}{|\mathbf{x}_Q - \mathbf{x}_P|} = \frac{\mathbf{n}^T (\mathbf{x}_Q - \mathbf{x}_P)}{|\mathbf{x}_Q - \mathbf{x}_P|} = \cos \theta_Q \quad (9)$$

where θ_Q is the angle between \mathbf{n} and the edge joining Q to P (see figure 3). Now write

$$F(\mathbf{n}) = \sum_{Q \in X_P} \left(\theta_Q - \frac{\pi}{2} \right)^2 \quad (10)$$

for the sum of the squares of the angles. This leads, however, to a non-linear minimization problem.

The following formulation of the angle square error does not suffer from this drawback and has proved to

be reliable and effective. Define

$$\tilde{h} = \frac{1}{m} \sum_{Q \in X_P} \hat{h}_Q \quad (11)$$

where, as before, $m = \text{card } X_P$ and let

$$H(\mathbf{n}) = \sum_{Q \in X_P} (\tilde{h} - \hat{h}_Q)^2 \quad (12)$$

Minimizing this error function then leads to the eigenvalue problem

$$B\mathbf{n} = \lambda\mathbf{n} \quad (13)$$

where

$$B = \sum_{Q \in X_P} (\tilde{\mathbf{x}} - \hat{\mathbf{x}}_Q)(\tilde{\mathbf{x}} - \hat{\mathbf{x}}_Q)^T \quad (14)$$

with

$$\hat{\mathbf{x}}_Q = \frac{\mathbf{x}_Q - \mathbf{x}_P}{|\mathbf{x}_Q - \mathbf{x}_P|}, \quad \tilde{\mathbf{x}} = \frac{1}{m} \sum_{Q \in X_P} \hat{\mathbf{x}}_Q \quad (15)$$

The choice of \mathbf{n} that minimizes the square error $H(\mathbf{n})$ is again given by the eigenvector associated with the smallest eigenvalue of the covariance matrix B .

4. CURVATURE ESTIMATION

The method adopted here for estimating surface curvatures and directions was first described by Hamann [6]; a similar approach has been presented by Frey [7, 8]. Define a local orthogonal coordinate system (x, y, z) whose origin is at P and such that the positive z axis lies in the direction of the normal \mathbf{n} at the point P . It follows that the x and y axes lie in the tangent plane. The height h_Q above the tangent plane of a point Q on the true surface can be expressed as a Taylor series in terms of derivatives evaluated at P and the displacements x and y . The leading terms of this Taylor series for h_Q are quadratic in x and y and equal to one half of the second fundamental form for the surface at P [9]. Let

$$z(x, y) = ax^2 + 2bxy + cy^2 \quad (16)$$

be the quadric surface formed by the leading terms of h_Q . If the coordinate axes x and y are aligned with the curvature directions \mathbf{t}_1 and \mathbf{t}_2 at the point P the quadric then assumes the form

$$z(x, y) = \frac{1}{2}\kappa_1 x^2 + \frac{1}{2}\kappa_2 y^2 \quad (17)$$

where κ_1 and κ_2 are the principal curvatures. This result may be exploited to compute estimates of the principal curvatures and curvature directions of the true surface that is represented by the triangulation. The paraboloid $z(x, y)$ is assumed to be a valid approximation over a region extending out to all points incident to P (*i.e.* for all $Q \in X_P$) and the coefficients a , b and c are then chosen so that $z(x, y)$ provides a

least squares fit to the set of heights $\{h_Q \mid Q \in X_P\}$ (see figure 4).

The surface triangulation is assumed to have a sufficient degree of regularity so that this approximation is reasonable. In particular, if \check{Q} is the projection of Q onto the tangent plane and if $\check{X}_P = \{\check{Q} \mid Q \in X_P\}$ then all the projected triangles formed by P and the points in \check{X}_P are required to have non-zero area and the correct orientation.

The points in X_P will not, in general, lie exactly on the paraboloid but for a sufficiently dense mesh this approximation of the curvatures at P can be expected to be reasonably accurate. The least squares formulation tends to smooth out the effects of any noise in the point positions.

The principal curvatures can be thus be obtained [6, 9] as $\kappa_1 = 2\lambda_1, \kappa_2 = 2\lambda_2$ where λ_1 and λ_2 are the eigenvalues of the symmetric matrix

$$C = \begin{pmatrix} a & b \\ b & c \end{pmatrix} \quad (18)$$

It follows that,

$$\kappa_1 = a + c - \Delta \quad , \quad \kappa_2 = a + c + \Delta \quad (19)$$

where

$$\Delta = [(a - c)^2 + 4b^2]^{\frac{1}{2}}. \quad (20)$$

The associated eigenvectors $\mathbf{t}_1, \mathbf{t}_2$ which lie in the tan-

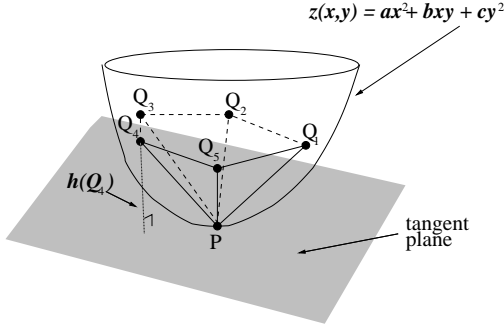


Figure 4: Paraboloid fit to the points in X_P .

gent plane of P give the orthogonal curvature directions relative to the local coordinate system (x, y, z) . These are found to be

$$\mathbf{t}_1 = \begin{pmatrix} -[\frac{\Delta - a + c}{2\Delta}]^{\frac{1}{2}} \text{sgn}(b) \\ [\frac{\Delta + a - c}{2\Delta}]^{\frac{1}{2}} \end{pmatrix} \quad (21)$$

and

$$\mathbf{t}_2 = \begin{pmatrix} [\frac{\Delta + a - c}{2\Delta}]^{\frac{1}{2}} \\ [\frac{\Delta - a + c}{2\Delta}]^{\frac{1}{2}} \text{sgn}(b) \end{pmatrix} \quad (22)$$

When all points in X_P are planar (*i.e.* all lying in the tangent plane at P) the coefficients a, b, c are all zero

in which case $\kappa_1 = \kappa_2 = 0$ and any pair of orthonormal vectors in the tangent plane can be taken as curvature directions. The remaining singular case occurs at an umbilic point ($\kappa_1 = \kappa_2 \neq 0$). In this case $a = c$ and $b = 0$ and any pair of orthonormal vectors in the tangent plane may again be taken as curvature directions.

It is interesting to investigate the conditions under which the rank of the covariance matrix for the least squares problem may be less than three, resulting in a set of equations whose solution is non-unique. Let $\{(x_i, y_i, z_i) \mid i = 1, \dots, m\}$ be the coordinates of the m points of X_P in the local orthogonal coordinate system. The least squares system has the form

$$G^T G \begin{pmatrix} a \\ b \\ c \end{pmatrix} = G^T \mathbf{z} \quad (23)$$

where

$$G = \begin{pmatrix} x_1^2 & x_1 y_1 & y_1^2 \\ \vdots & \vdots & \vdots \\ x_m^2 & x_m y_m & y_m^2 \end{pmatrix} \quad (24)$$

Since $\text{rank } G^T G = \text{rank } G$ it is convenient to examine the matrix G and determine the conditions that lead to linear dependencies among its columns and rows. Suppose first that the columns are linearly dependent so that there exist constants α and β such that

$$\alpha x_i^2 + \beta x_i y_i + y_i^2 = 0, \quad \forall i = 1, \dots, m \quad (25)$$

This can only occur if $y_i = r x_i$ for all $i = 1, \dots, m$, where r is a real root of the equation $r^2 + \beta r + \alpha = 0$. In other words, the coordinates (x_i, y_i) of all the projected points in \check{X}_P lie on a straight line through the origin (*i.e.* through the point P). This is clearly not possible since it implies that all the projected triangles formed by P and the points of \check{X}_P have zero area.

Now suppose that rows i, j and k are linearly dependent so that there exist constants α and β such that

$$\begin{pmatrix} x_i^2 & x_j^2 & x_k^2 \\ x_i y_i & x_j y_j & x_k y_k \\ y_i^2 & y_j^2 & y_k^2 \end{pmatrix} \begin{pmatrix} \alpha \\ \beta \\ 1 \end{pmatrix} = \begin{pmatrix} 0 \\ 0 \\ 0 \end{pmatrix} \quad (26)$$

This implies that the determinant of the Vandermonde matrix

$$V = \begin{pmatrix} x_i^2 & x_j^2 & x_k^2 \\ x_i y_i & x_j y_j & x_k y_k \\ y_i^2 & y_j^2 & y_k^2 \end{pmatrix} \quad (27)$$

is zero. But

$$\det V = (x_i y_j - x_j y_i)(x_i y_k - x_k y_i)(x_j y_k - x_k y_j) \quad (28)$$

Thus $\det V = 0$ and a linear dependence of these three rows exists if the local (x, y) coordinates of at least two of the points in \check{X}_P lie on a straight line through P . No more than two of the projected points may lie on

any particular straight line through P since otherwise there would be at least one projected triangle with zero area. Note also that if two projected points $\check{Q}, \check{R} \in \check{X}_P$ lie on a straight line through P then they must necessarily lie on opposite sides of P (see figure 5 for an example of a configuration with $m = 4$ and two pairs of projected points $(\check{Q}_1, \check{Q}_3)$ and $(\check{Q}_2, \check{Q}_4)$ that lie on straight lines through P).

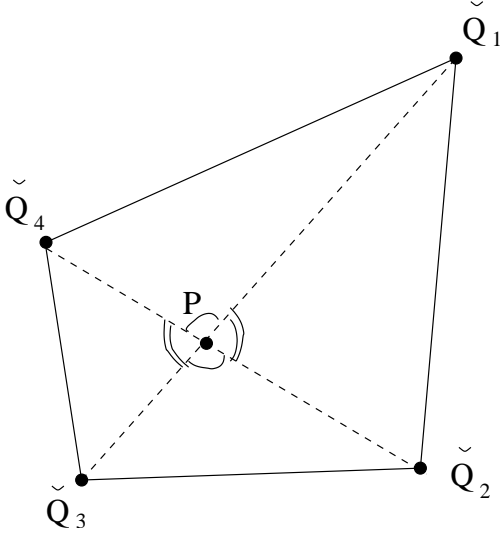


Figure 5: Projected point pairs $(\check{Q}_1, \check{Q}_3)$ and $(\check{Q}_2, \check{Q}_4)$ each lie on a straight line through P .

It follows that the number of linearly independent rows, and hence the rank of G , must be three if $m \geq 5$ leading to a non-singular least squares system. The $m = 4$ case will also be non-singular unless the four projected points in \check{X}_P consist of two pairs that lie on straight lines through P (see, for example, figure 5). The $m = 3$ case will always be non-singular if the surface triangulation is a closed manifold. If the manifold is not closed and P lies on the boundary then the $m = 3$ case will be singular if two of the three points in \check{X}_P lie on a straight line through P .

Define P to be an interior point if it does not lie on the manifold boundary (if the surface triangulation is a closed manifold then all points are interior). The above results can be stated as

Theorem: Let P be an interior point of a surface triangulation, X_P the set of edge incident points to P and let T_P be the associated tangent plane. The least squares estimate of the principal curvatures at P always has a unique solution if the valence of P is either 3 or greater than 4. If the valence of P is 4 then there will be a unique solution unless the projection of X_P onto T_P consists of two pairs of points such that each pair lies on a line passing through the point P .

If the singular case arises, the least squares problem can be resolved by using the pseudo-inverse to determine the coefficients a , b and c of the approximating paraboloid.

5. SURFACE POINT PROJECTION

Enrichment of the surface triangulation is carried out by inserting a new mesh point at the midpoint of the longest edge for any surface triangle that has been tagged for refinement. The surface triangle is thus replaced by two new triangles. Whenever the surface triangulation is associated with a conforming volume mesh of tetrahedra the tetrahedra incident to the split edge are simultaneously divided into new tetrahedra so as to create a modified mesh that contains the new point [10]. When the mesh is coarsened by edge collapse it is possible for the two edge endpoints to be replaced by a new point at the midpoint of the collapsed edge. In order to maintain the surface geometry during enrichment and/or coarsening of the surface triangulation it is therefore necessary to project the point from the midpoint of the original surface edge onto the underlying surface [10]. The manner by which the point is projected depends on whether or not the edge lies on a feature curve.

For a non-feature edge let the two endpoints of be P_0 with position vector \mathbf{x}_0 and P_1 with position vector \mathbf{x}_1 , and let the unit normals at these points be \mathbf{n}_0 and \mathbf{n}_1 respectively. Let \mathbf{n} be the unit normal to the plane in which the new point Q should lie, usually chosen to be the plane that bisects the dihedral angle between the two boundary triangles incident to the edge joining P_0 and P_1 . This plane also contains the points P_0 and P_1 and thus the edge joining P_0 to P_1 . Then fit a cubic polynomial lying in the plane through the points P_0 and P_1 whose tangents at P_0 and P_1 are parallel to the corresponding surface tangent planes. Let \mathbf{c} be the vector from the edge midpoint to the point Q which lies halfway along the interpolating cubic curve. The correction \mathbf{c} thus represents a displacement in the plane that should be added to the coordinates of the edge midpoint in order to obtain an approximation to the true boundary surface. This quadratic recovery procedure based on Hermite interpolation has been previously described by Löhner [12]. It should be noted, however, that the expression for the correction \mathbf{c} assumes a particularly simple form when the projection is applied, as here, at the midpoint of the edge joining P_0 and P_1 .

The tangent vectors \mathbf{t}_0 and \mathbf{t}_1 that lie in the desired plane are

$$\mathbf{t}_0 = \frac{\mathbf{n}_0 \times \mathbf{n}}{|\mathbf{n}_0 \times \mathbf{n}|}, \quad \mathbf{t}_1 = \frac{\mathbf{n}_1 \times \mathbf{n}}{|\mathbf{n}_1 \times \mathbf{n}|} \quad (29)$$

Let α_0 be the angle between \mathbf{t}_0 and the edge vector

$\mathbf{x}_1 - \mathbf{x}_0$. Similarly, define α_1 as the angle between \mathbf{t}_1 and $\mathbf{x}_1 - \mathbf{x}_0$ and let $m_0 = \tan\alpha_0$, $m_1 = \tan\alpha_1$, be the imposed slopes of the interpolating curve at each endpoint. The displacement is then given by

$$\mathbf{c} = \frac{(m_0 - m_1)}{8} \mathbf{n} \times (\mathbf{x}_1 - \mathbf{x}_0) \quad (30)$$

For a feature edge the normal at each endpoint is not uniquely defined and an alternative interpolation procedure must be adopted. In this case, a cubic polynomial is interpolated through the points P_0 and P_1 and the two neighboring points, one on each side of P_0 and P_1 . If either P_0 or P_1 is a terminus point for the feature then the interpolating points are changed appropriately to fit a one side cubic polynomial.

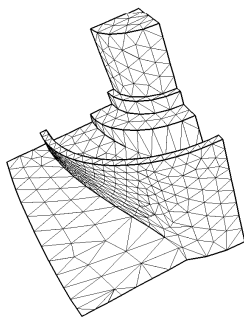


Figure 6: Surface triangulation for a mechanical object.

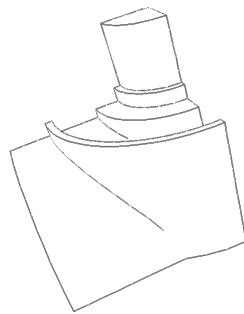


Figure 7: Feature edges for the mechanical object.

6. RESULTS

6.1 Feature detection

Figure 7 shows the set of curves that were found by the feature identification algorithm for a mechanical object. Figure 6 shows the surface triangulation from

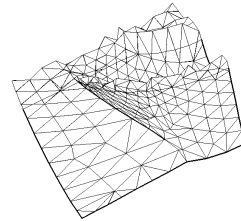


Figure 8: Cut through the mechanical object showing the tetrahedral mesh.

which the feature edges forming these curves were extracted. It is apparent from figure 6 that most features on this object are unambiguously defined. This example therefore represents a relatively simple test for which an effective feature extraction method should not experience any difficulty in finding the majority of feature curves. It is also reasonable to assume that this example would be relatively insensitive to the choice of user defined constants. The constants that were used for all the cases shown in this paper are $\phi = 30^\circ$, $\lambda = 2$ and $\mu = 0$. Figure 8 shows a cut through this mechanical object to display some of the tetrahedra that form a volume mesh throughout its interior.

A more challenging example for which the feature curves are not so well defined is presented in figure 9 which shows a surface triangulation of a pig. The identification of features in this case is a highly subjective exercise. Indeed, if the triangulation were sufficiently fine for the underlying surface to be captured to a high degree of smoothness then it would be reasonable to regard the object as being devoid of features. The number of feature curves that are actually detected will therefore depend on the fineness of the triangulation in addition to the values set for the user defined constants. Figure 10 shows the feature curves that were identified for the triangulation shown in figure 9 and for the constants assumed here ($\phi = 30^\circ$, $\lambda = 2$, $\mu = 0$). The broad outline of the animal is evident although it could perhaps be mistaken for a dog based on the feature curves alone. Figure 11 presents a cut through the pig to show some of the tetrahedra covering the interior.

6.2 Enrichment and Coarsening

The feature extraction algorithm has been combined with a suite of routines for adapting tetrahedral meshes [10]. These adaptation routines carry out coarsening and enrichment of meshes as well as im-

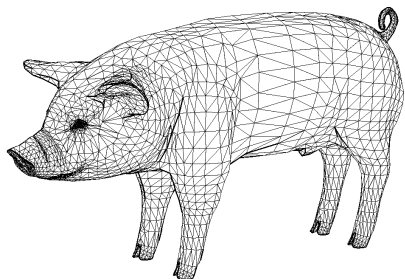


Figure 9: Surface triangulation for a pig.



Figure 10: Feature edges for the pig.

proving mesh quality through a variety of edge/face swaps. Additional routines monitor mesh quality in order to trigger mesh adaptation that will recover a good quality mesh following any mesh movement associated with time evolving domains [11]. Figures 12 and 13 show the surface triangulation and a cut through the associated tetrahedral mesh for the mechanical object after enrichment to increase the number of surface points by a factor of four. Figures 14 and 15 show the corresponding views after coarsening has been applied to reduce the number of original surface points to about 50% of the original number.

Figures 16 and 17 show the surface triangulation and a cut through the associated tetrahedral mesh for the pig after enrichment. Finally, figures 18 and 19 show corresponding views of the pig after coarsening has been applied.

7. ACKNOWLEDGMENT

Part of this research was carried out in the course of consulting activity for Combustion Research and Flow Technology, Inc. and was funded by the Air Force Research Laboratory, Wright-Patterson AFB, OH under

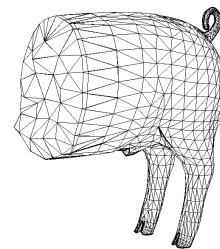


Figure 11: Cut through the pig showing the tetrahedral mesh.

contract F33615-02-C-3215, Phase II SBIR (technical monitors Frank Witzeman and Matthew Grismer). The support is gratefully acknowledged.

References

- [1] J. CANNY A computational approach to edge detection, *IEEE Trans. Pattern Analysis and Machine Intelligence*, Vol. **PAMI-8**, No. 6, pp. 679-696, 1986
- [2] W. SCHRÖDER, J. ZARGE AND W. LORENSEN Decimation of triangle meshes, *Proc. SIGGRAPH 92*, pp. 65-70, 1992
- [3] M. GARLAND AND P.S. HECKBERT Surface simplification using quadric error metrics, *Proc. SIGGRAPH 97*, pp. 209-216, 1997
- [4] A. HUBELI, K. MEYER AND M. GROSS Mesh edge detection, *Technical Report 351*, ETH Zürich, Dept. of Computer Science, 2000
- [5] X. JIAO AND M.T. HEATH Feature detection for surface meshes, *Proc. 8th International Conference on Numerical Grid Generation*, Honolulu, HI, June 2002
- [6] B. HAMANN Curvature approximation for triangulated surfaces, *Computing Suppl.*, Vol. **8**, pp. 139-153, 1993
- [7] P.J. FREY AND H. BOROUCAKI Surface mesh quality evaluation, *Int. J. Numer. Meth. Engng.*, Vol. **45**, pp. 101-118, 1999
- [8] P.J. FREY About surface remeshing, *9th International Meshing Roundtable*, New Orleans, 2000
- [9] D.J. STRUIK *Lectures on Classical Differential Geometry*, pub. Dover, ISBN 0-486-65609-8, 1988

- [10] T.J. BAKER Mesh deformation and modification for time dependent Problems, *Int. J. Num. Meth. Fluids*, Vol. **43**, pp. 747-768, 2003
- [11] T.J. BAKER Mesh movement and metamorphosis, *10th International Meshing Roundtable*, Newport Beach, CA, 2001, also in *Engineering with Computers*, Vol. **18**, pp. 188-198, 2002
- [12] R. LÖHNER Regriding Surface Triangulations, *JCP*, Vol. **126**, pp. 1-10, 1996

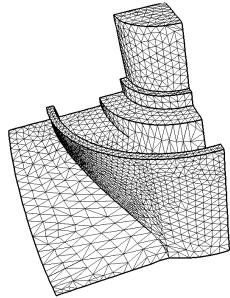


Figure 12: Surface triangulation of the mechanical object after mesh enrichment.

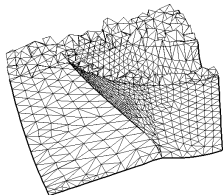


Figure 13: Cut through tetrahedral mesh for the enriched mechanical object.

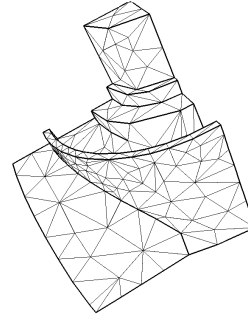


Figure 14: Surface triangulation of the mechanical object after mesh coarsening.

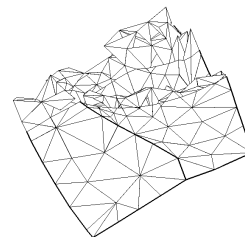


Figure 15: Cut through tetrahedral mesh for the coarsened mechanical object.

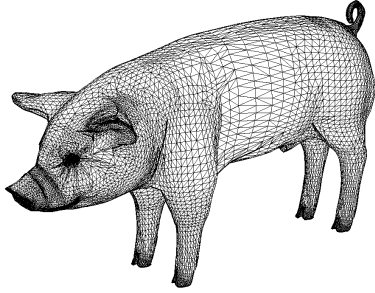


Figure 16: Surface triangulation for the pig after mesh enrichment.

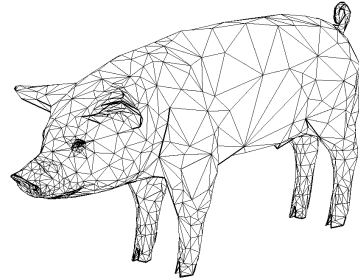


Figure 18: Surface triangulation for the pig after mesh coarsening.

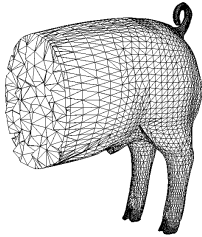


Figure 17: Cut through tetrahedral mesh for the pig after mesh enrichment.

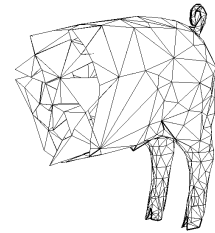


Figure 19: Cut through tetrahedral mesh for the pig after mesh coarsening.